Article

Chinese Science Bulletin

Materials Science

March 2011 Vol.56 No.8: 796–802
doi: 10.1007/s11434-010-4300-3

Effect of Co on the martensitic transformation, crystal structure and magnetization of $Ni_{52.5}Mn_{23.5}Ga_{24}$ based ferromagnetic shape memory alloys

YAN ShaoMeng, PU Jian, CHI Bo & LI Jian*

School of Materials Science and Engineering, State Key Laboratory of Material Processing and Die & Mould Technology, Huazhong University of Science & Technology, Wuhan 430074, China

Received August 11, 2010; accepted November 24, 2010

Five $(Ni_{52.5}Mn_{23.5}Ga_{24})_{100-x}Co_x$ (x = 0, 2, 4, 6, 8) alloys were prepared by arc melting, and the effects of Co addition on the martensitic phase transformation, crystal structure and magnetization were investigated. The phase transformation temperatures M_s, M_f, A_s and A_f are proportional to the content of Co in the $(Ni_{52.5}Mn_{23.5}Ga_{24})_{100-x}Co_x$ alloys, which appears to be due to the variation in the valance electron concentration. The Curie temperature is sensitive to the composition of the alloy. As the amount of Co changes, both the Co-Mn exchange interaction and the distance between Mn atoms change. These, in turn, affect the Curie temperature and magnetization behavior of the alloy. The martensite phases in all the alloys are domained in three different orientations, the domain boundary was determined to belong to the family of {1 1 2} lattice planes.

Ni-Mn-Ga alloy, Martensitic transformation, domain boundary, Curie temperature, magnetization

Citation: Yan S M, Pu J, Chi B, et al. Effect of Co on the martensitic transformation, crystal structure and magnetization of $Ni_{52.5}Mn_{23.5}Ga_{24}$ based ferromagnetic shape memory alloys. Chinese Sci Bull, 2011, 56: 796–802, doi: 10.1007/s11434-010-4300-3

Ferromagnetic shape memory alloys (FSMAs) are under investigation for application as a new type of actuator material that combines the property of ferromagnetism with the shape memory effect associated with reversible martensitic transformations [1–4]. The most interesting member of the FSMA is the Heusler alloy, a known group of ternary intermetallic compounds with a stoichiometric composition of A_2BC. The A element can be Fe, Cr, Ni, Co or Cu; the B element can be Mn, Zr, Ti or Nb and the C can be Al, Sn, Ga, In or Sb. Because the Heusler alloy possesses both thermoelastic martensitic transformations and ferromagnetic transitions, the martensitic transformation strain is much larger than those demonstrated by magnetostrictive materials when exposed to a magnetic field, demonstrating that the shape memory effect can be controlled with an applied magnetic field as well as by variations in temperature.

Ni_2MnGa based Heusler alloys have a faster response to a magnetic field than thermally controlled shape memory alloys [5,6], which makes them highly interesting for many novel technological applications especially as actuators [7,8]. The induced strain from the magnetic field forces a rearrangement of the crystallographic orientation of the martensitic variants formed during the thermoelastic martensitic transformation [9]. The martensitic transformation start temperature, M_s, of a Ni_2MnGa based alloy is strongly depended on its composition; the Curie temperature (T_C) is, however, less sensitive [10]. The temperature range for producing the magnetic field induced strain, which can be up to 10% of the value, is determined by the M_s and T_C and can be optimized for specific applications by changes in the alloy composition.

Other than the elements Fe [11–13], Y [14], Cu [15,16], Gd [17], Nb [18] and others, which have been confirmed to affect the characteristics of these Ni-Mn-Ga Heusler alloys, the ferromagnetic 3d transition element Co has been frequently used to modify phase transformation temperatures,

*Corresponding author (email: lijian@hust.edu.cn)

Curie point, magnetic and mechanical properties [13,19–21]. In the present study, a Ni-Mn-Ga alloy, with a composition of 52.5 at% Ni, 23.5 at% Mn and 24 at% Ga and martensitic phase transformation temperatures near the room temperature [22] was selected as the baseline alloy; various Co contents were added to this alloy and the effect of this Co addition on martensitic transformation, crystal structure and magnetization of the $Ni_{52.5}Mn_{23.5}Ga_{24}$ alloy was systematically investigated.

1 Experimental

Five $Ni_{52.5}Mn_{23.5}Ga_{24}$ based alloys with various amounts of added Co were prepared from 99.95 wt% pure elemental metals by arc-melting under an argon atmosphere. Each ingot was melted five times to ensure homogeneity; and finally the melted alloy was suck-cast into a water-cooled cylindrical copper mold placed at the bottom of the arc furnace to form an alloy rod with a constant diameter of 3 mm. The alloys contained 0, 2, 4, 6 or 8 at% of Co, in terms of the baseline $Ni_{52.5}Mn_{23.5}Ga_{24}$, and have been designated NMG-C0, NMG-C2, NMG-C4, NMG-C6 and NMG-C8, respectively. The alloy rods were annealed in evacuated quartz tubes at 1000°C for 24 h for further homogenization. The chemical compositions of the alloys were analyzed using an X-ray fluorescence spectroscope (EAGLE III), as listed in Table 1. The analyzed composition deviates from the intended content because of element volatilization, especially for Mn and Co, during alloy preparation and homogenization.

Disc specimens for further examination were obtained by slicing the rods with a low-speed diamond saw (WEIYI-DTQ™ 5). The optical metallographic samples were prepared by wet polishing the discs, followed by etching with a solution of 25 mL HNO_3-75 mL ethanol. The phase transformation characteristic temperatures were determined in a differential scanning calorimeter (DSC, Perkin-Elmer diamond), and the Curie temperature was determined using a thermogravimetric analyzer (TGA 29500) with an applied magnetic field. Both the heating and cooling rates used in the above analyses were 10 K min^{-1}. The crystal structure of the sample powder was identified by X-ray diffraction (XRD) using an X'Pert PRO diffractometer with Cu K_α radiation. Magnetization hysteresis loops were measured with a vibrating sample magnetometer (VSM, JAAM-2000C). A transmission electron microscope (TEM, FEI Tecnai G2-20) was employed to characterize the domained martensitic phase. The thin foil specimens for TEM examination were prepared by mechanically polishing and ion milling (GATAN-691).

2 Results and discussion

2.1 Phase transformation temperatures

Figure 1 shows the DSC curves for all the alloys prepared. It can be seen that there is only one endothermic and one exothermic peak in the course of heating and cooling, respectively, indicating a typical one-step thermoelastic martensitic transformation occurs in all of the NMG-Cx (x = 0, 2, 4, 6 and 8) alloys. The exothermic and endothermic peaks are associated with the martensitic transformation during cooling and the austenitic transformation upon heating. The compositional effect caused by Co doping on the phase transformation temperatures is shown in Figure 2, where M_s is the martensitic transformation start temperature, M_f is the martensitic transformation finish temperature, A_s is the austenitic transformation start temperature and A_f is the austenitic transformation finish temperature. The insert in Figure 1 shows how the characteristic temperatures were obtained. The phase transformation temperatures increase linearly as the Co content increases. The relationship between the phase transformation temperatures and the Co content X_{Co} in the alloy NMG-Cx (x = 0, 2, 4, 6 and 8) can

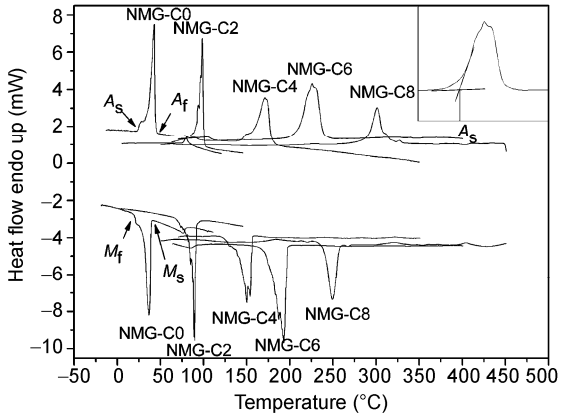

Figure 1 DSC curves of the NMG-Cx (x = 0, 2, 4, 6 and 8) alloys during heating and cooling at a rate of 10 K/min. The insert explains how the transformation temperatures have been determined.

Table 1 The chemical composition of the prepared alloys as determined by XRF compared with the nominal composition (values in bracket)

Alloy	Ni (at %)	Mn (at %)	Ga (at %)	Co (at%)
NMG-C0	53.23 (52.50)	22.33 (23.50)	24.44 (24.00)	0 (0)
NMG-C2	52.17 (51.45)	22.05 (23.03)	23.74 (23.52)	2.05 (2)
NMG-C4	51.13 (50.40)	21.61 (22.56)	23.30 (23.04)	3.96 (4)
NMG-C6	49.96 (49.35)	20.06 (22.09)	23.03 (22.56)	5.95 (6)
NMG-C8	48.97 (48.30)	20.50 (21.62)	22.70 (22.08)	7.83 (8)

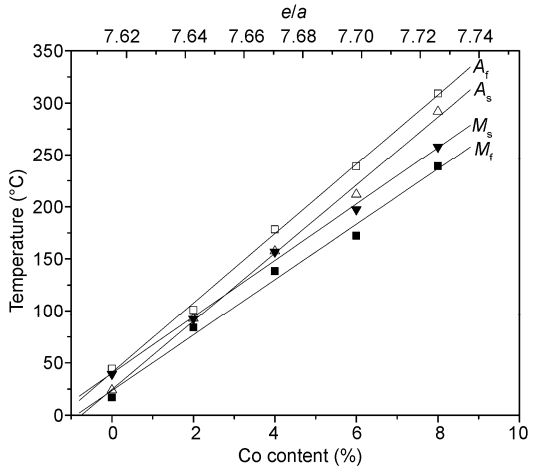

Figure 2 Dependence of phase transformation temperatures M_s, M_f, A_s and A_f on Co addition and the valance electron concentration *e/a* in the $Ni_{52.5}Mn_{23.5}Ga_{24}$ base alloy.

be expressed as

$$M_s\ (°C)=40.02+27.13X_{Co}, \quad (1)$$

$$M_f\ (°C)=23.59+26.62X_{Co}, \quad (2)$$

$$A_s\ (°C)=24.59+32.74X_{Co}, \quad (3)$$

$$A_f\ (°C)=40.90+33.36X_{Co}, \quad (4)$$

with correlation coefficients higher than 0.99.

It is widely accepted that the valance electron concentration, *e/a*, affects the transformation temperature in Ni-Mn-Ga alloys [23,24]. The number of valence electrons is assumed to be 10 for Ni, 7 for Mn, 3 for Ga and 9 for Co. The addition of Co to the baseline alloy $Ni_{52.5}Mn_{23.5}Ga_{24}$ increases the *e/a* ratio, and, in turn, increases the phase transformation temperatures, as also shown in Figure 2. The thermal hysteresis of the phase transformation, the difference between A_f and M_s, is increased as the Co content increases. Thermodynamically the degree of thermal hysteresis is proportional to the elastic energy caused by martensite formation in the austenite matrix [25], which suggests that the elastic energy accompanied with the formation of martensite is gradually increased with the addition of Co into the $Ni_{52.5}Mn_{23.5}Ga_{24}$ alloy.

2.2 Crystal structure of the martensite phase

Figure 3 presents the indexed XRD patterns of the NMG-C*x* (*x* = 0, 2, 4, 6 and 8) alloys at room temperature. This confirms that the non-modulated martensite is the only phase in the NMG-C2, NMG-C4, NMG-C6 and NMG-C8 alloys, and that martensite and austenite coexist in NMG-C0. According to the DSC-derived results (Figure 1), all the characteristic temperatures of phase transformation of the NMG-C2, NMG-C4, NMG-C6 and NMG-C8 alloys are well beyond room temperature, at which the XRD was conducted, whereas those for the NMG-C0 are in the vicinity of room temperature, particularly A_s and M_f. Therefore, the XRD results are consistent with the DSC results. Table 2 lists the calculated lattice parameters *a* and *c* of the martensite phase in all the prepared alloys based on the XRD results. A tetragonal crystal structure in the space group I4/mmm is confirmed, which agrees with that reported for Ni-Mn-Ga-Co alloys [26]. The atomic radius of Ni, Mn and Ga is 0.162, 0.179 and 0.181 nm, respectively; Co (atomic radius 0.167 nm) may substitute more for Ni than for Mn and Ga in the lattice in view of the difference of atomic radius, as suggested by the variations in alloy composition (Table 1). This may results in lattice expansion along the *c* axis and contraction along the *a* and *b* axes; consequently, the tetragonal ratio *c/a* gradually increases with the addition of Co, without significantly changing the volume of the unit cell (Table 2). Such changes in the lattice parameters caused by Co addition originate in the variation of the valance electron concentration and are an important factor that affects the martensitic transformation, magnetic anisotropy, mechanical properties and the theoretical maximum of the magnetic shape memory effect [27]. The gradual reduction in the XRD intensity as the Co content increases, as shown in Figure 3, may be due to the lower scattering factor of Co than Ni and Ga and that the addition of Co increases the disorder of atoms in the Ni-Mn-Ga alloys.

2.3 Microstructure and crystallographic orientation of martensite

Figure 4 shows a typical microstructure of the NMG-C*x* (*x* = 0, 2, 4, 6 and 8) alloys and reveals that the alloys with

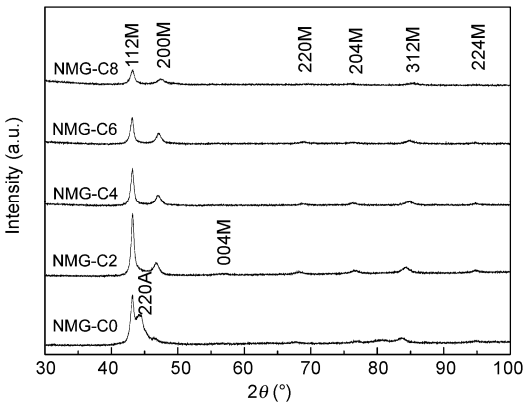

Figure 3 Indexed XRD patterns of the NMG-Cx (x = 0, 2, 4, 6 and 8) alloys at room temperature, "A" and "M" with the index stand for austenite and martensite phases, respectively.

Table 2 Lattice parameters of the martensite in various alloys prepared

Alloy	*a*(Å)	*c*(Å)	*c/a*	Vol. (Å^3)
NMG-C0	3.916	6.418	1.639	98.420
NMG-C2	3.888	6.470	1.665	97.804
NMG-C4	3.859	6.542	1.696	97.423
NMG-C6	3.855	6.558	1.702	97.459
NMG-C8	3.831	6.582	1.719	96.601

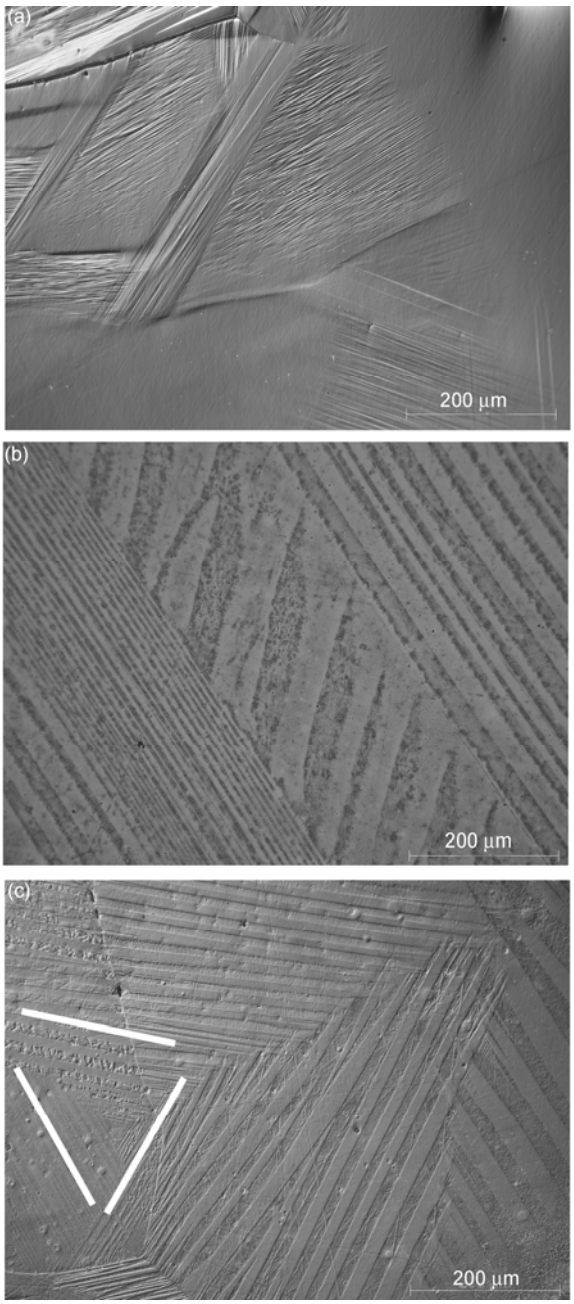

Figure 4 Typical optical microstructure of (a) NMG-C0, mixed austenite and martensite; (b) NMG-C2 and (c) NMG-C8, single-phase martensite at room temperature.

added Co contain a domained martensite phase at room temperature; however, the alloy without Co gives a dual-phase microstructure comprised of martensite and austenite. This observation agrees with what suggested by the DSC and XRD results. The M_s, A_s and M_f and A_f temperatures of the NMG-C0 alloy are 39, 24, 17 and 44°C, respectively, and subtle fluctuations in room temperature will lead to a meaningful change of the volume fractions of martensite and austenite in it.

It can also be noted from Figure 4 that the martensite phase is self-accommodated in a lamellar configuration. It is known that the parent austenite phase belongs to the space group Fm-3m [28] with a cubic crystal structure, and the product martensite phase belongs to the space group I4/mmm with a tetragonal crystal structure. The transformation is therefore from a cubic to a tetragonal structure. This means three martensite variants are expected which can be represented by three lattice deformation matrices U_1, U_2 and U_3, as described in [29]. When the variants meet each other in space, three different specific arrangements, i.e. U_1-U_2, U_2-U_3 and U_3-U_1, are required to achieve elastic energy minimization. This explains the observation of three lamellar clusters in three different directions when there is no external stress in the grain, as seen in Figure 4(c).

Figure 5 is a bright-field TEM image of the NMG-C8 alloy at room temperature and the selected area electron diffraction (SAED) pattern at the conjunction of two lamellar martensite variants. Under the extreme magnification of TEM, it can be observed that the lamellar martensite features an even finer striped substructure, similar to what reported in [30–32]. However, only one set of diffraction spots was generated from the lamellar martensite. The reason for this phenomenon needs to be further understood. The SAED patterns at the conjunction of two lamellar martensites (Figure 5(b) and (c)) yields two sets of diffraction spots originated from each martensite lamella obtained and indexed with respect to the zone axes of $[0\ 2\ -1]^{I}$ ($[2\ 0\ -1]^{II}$) and $[-1\ 1\ 0]^{I}$ ($[1-1\ 0]^{II}$). Thus, the $[0\ 2\ -1]^{I}$ and $[-1\ 1\ 0]^{I}$ directions of the lamella I are parallel to the $[2\ 0\ -1]^{II}$ and $[1\ -1\ 0]^{II}$ directions of the lamella II, respectively. According to these results, the interface between lamellae I and II is determined as $(1\ 1\ 2)^{I}$ or $(-1\ -1\ -2)^{II}$. Therefore, it can be concluded that the lamellar martensite in the Co doped Ni-Mn-Ga alloys is twinned with the {1 1 2} lattice planes as the twin boundary, and the atomic arrangement of the twinned martensite is assumed to be that shown in Figure 6.

2.4 Curie temperature and magnetization

Figure 7(a) shows the results of thermogravimetric measurement of the NMG-Cx (x = 0, 2, 4, 6 and 8) alloys over

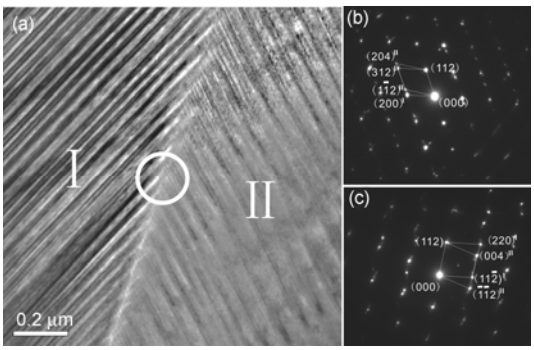

Figure 5 (a) TEM bright field image of the NMG-C8 alloy and selected area electron diffraction patterns from the circled area with respect to (b) $[0\ 2\ -1]^{I}$ ($[2\ 0\ -1]^{II}$) and (c) $[-1\ 1\ 0]^{I}$ ($[1\ -1\ 0]^{II}$) zone axes.

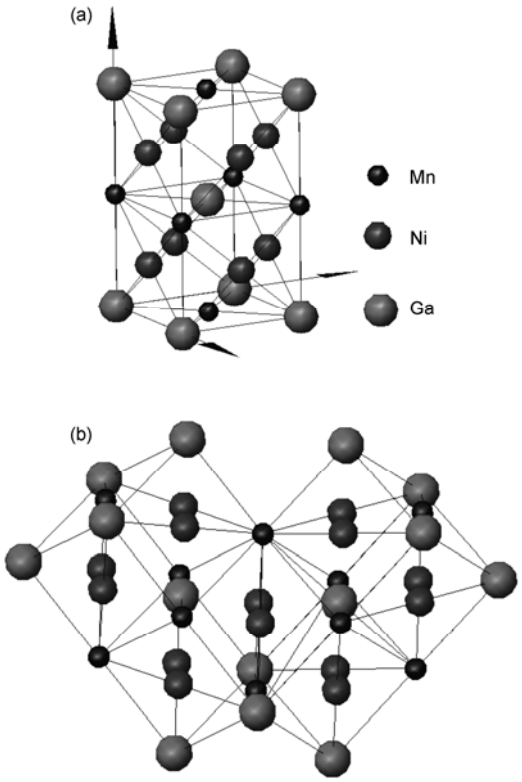

Figure 6 Atomic arrangement of Ni_2MnGa martensite in the space group I4/mmm: (a) Single variant; (b) twinned variants.

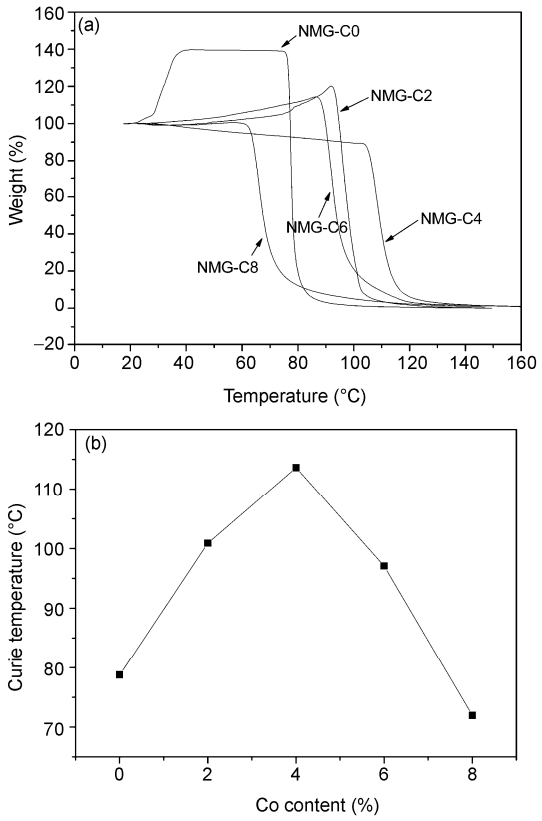

Figure 7 Thermogravimetric measurement of the NMG-Cx (x = 0, 2, 4, 6 and 8) alloys (a) and the dependence of the Curie temperature T_C on the Co content (b).

the temperature range 20 to 200°C under a constant applied magnetic field. The temperature at which abrupt weight loss starts corresponds to the Curie point T_C. The dependence of T_C on the content of Co added to the NMG-Cx alloys is shown in Figure 7(b). T_C increases from 79°C in NMG-C0 to a maximum of 114°C at x = 4 (NMG-C4), then decreases with x to 71°C in NMG-C8. For the alloys NMG-C0 and NMG-C2 with T_C higher than A_f, the ferromagnetic transition occurs in the austenite phase whereas the alloys NMG-C4, MNG-C6 and NMG-C8 which have a T_C lower than M_f, the ferromagnetic transition occurs in the martensite phase. It seems that T_C is sensitive to Co addition; however, no direct relationship between T_C and Co addition or the valance electron concentration *e/a* can be established. It is well known that the ferromagnetism of the Ni-Mn-Ga alloys originates from the ferromagnetic coupling between Mn atoms [33], with some contribution from the Ni-Mn interactions [10]. Accordingly, the effect of the doping element on the ferromagnetism of the Ni-Mn-Ga alloys can be categorized into two aspects: (1) changing the Mn-Mn interaction by increasing the Mn-Mn distance or Mn dilution and (2) introducing other stronger ferromagnetic interactions to substitute for the Ni-Mn coupling. In all the NMG-Cx (x = 0, 2, 4, 6 and 8) alloys prepared, Mn dilution is not a significant factor, as seen in Table 1, and its contribution to the ferromagnetism is expected to be negligible.

However, the Ni content decreases noticeably as the Co content increases, resulting in stronger Co-Mn interactions. This accounts for the T_C increasing from 79°C in NMG-C0 to 101°C in NMG-C2, when the T_C occurs in the austenite phase. With further addition of Co, the martensitic transformation increases and the martensite becomes more tetragonal, leading to a longer average Mn-Mn distance. Such Mn-Mn distance change counteracts the Co-Mn coupling contribution and decreases the Curie temperature from 114°C in NMG-C4 to 71°C in NMG-C8.

The magnetization curves of the prepared alloys at room temperature (~13°C on the day of measurement) are presented in Figure 8, with all the specimens in the martensite state. The magnetization hysteresis loops were measured following a magnetization sequence of 0 kOe→15 kOe→ –15 kOe→15 kOe. The magnetization curve from each alloy is highly reversible with a very small coercive force (H_c) of less than 200 Oe, exhibiting a typical soft magnetization behavior. It can be seen that the saturation magnetization decreases continuously with Co addition from 85 emu/g for NMG-C0 to 35 emu/g for NMG-C8, and the saturation magnetic field is also lowered from 10 to 4 kOe, correspondingly. This result is different from that obtained in Co-doped Ni-Fe-Ga alloys [34] where the saturated magnetization increased with the addition of Co. As discussed

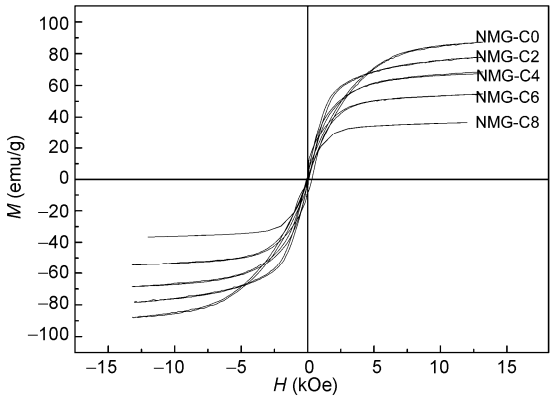

Figure 8 Magnetization curves of the NMG-Cx (x = 0, 2, 4, 6 and 8) alloys at room temperature (~13°C).

above, the magnetic moment of the Ni-Mn-Ga Heusler alloy originates in the indirect exchange interaction between Mn atoms. The intrinsic magnetic properties, such as the Curie temperature and saturation magnetization, are primarily determined by the Mn-Mn atom distance [33,35]. As can be seen from Table 2, Co addition from 0 to 8% in the NMG-Cx (x = 0, 2, 4, 6 and 8) alloys, makes the martensite phase more tetragonal and consequently the Mn-Mn distances increase on average. This may explain why the saturation magnetization is lowered with Co addition. Partial Co substitution for Mn may also play a role in the decrease in magnetization.

3 Conclusions

From the present study, the following conclusions can be made:

(1) In the $(Ni_{52.5}Mn_{23.5}Ga_{24})_{100-x}Co_x$ (x =0, 2, 4, 6 and 8) alloys, the phase transformation temperatures M_s, M_f, A_s and A_f increase linearly with Co addition in the alloys, with the valance electron concentration determining the dependence of the phase transformation temperatures on the Co content.

(2) The Curie temperature is sensitive to the composition of the alloys, with the Co-Mn exchange coupling and the distance between Mn atoms determining the dependence of the Curie temperature and magnetization behavior in austenite and martensite phases, respectively.

(3) The martensite phase in all the alloys is domained with three different orientations determined by the nature of the cubic to tetragonal transformation from austenite to martensite. The domain boundary belongs to the {112} family of lattice planes.

The authors would like to express their sincere gratitude to the Analytical and Testing Center of Huazhong University of Science and Technology for TEM and XRD assistance.

1 Sozinov A, Likhachev, A A, Lanska N, et al. Giant magnetic-field-induced strain in NiMnGa seven-layered martensitic phase. Appl Phys Lett, 2002, 80: 1746–1748
2 Brown P J, Crangle J, Kanomata T, et al.The crystal structure and phase transitions of the magnetic shape memory compound Ni_2MnGa. J Phys-Condensed Matter, 2002, 14: 10159–10171
3 Pons J, Chernenko V A, Santamarta R, et al. Crystal structure of martensitic phases in Ni-Mn-Ga shape memory alloys. Acta Mater, 2000, 48: 3027–3038
4 Koyama K, Kanomata T, Kainuma R, et al. High-field X-ray diffraction measurements of novel ferromagnetic shape-memory alloy $Ni_{50}Mn_{36}Sn_{14}$. Physica B: Condensed Matter, 2006, 383: 24–25
5 Nie Q, Ji Z Y, Lin J X, et al. Surface nanostructures orienting self-protection of an orthodontic nickel-titanium shape memory alloys wire. Chinese Sci Bull, 2007, 52: 3020–3023
6 Liang C Y, Yang Y, Wang H S, et al. Preparation of porous microstructures on NiTi alloy surface with femtosecond laser pulses. Chinese Sci Bull, 2008, 53: 700–705
7 Ullakko K, Huang J K, Kantner C, et al. Large magnetic-field-induced strains in Ni_2MnGa single crystals. Appl Phys Lett, 1996, 69: 1966–1968
8 Bhattacharya K, James D R. The material is the machine. Science, 2005, 307: 53
9 O'Handley R C, Murray S J, Marioni M, et al. Phenomenology of giant magnetic-field-induced strain in ferromagnetic shape-memory materials. J Appl Phys, 2000, 87: 4712–4717
10 Khovailo V V, Chernenko V A, Cherechukin, A A, et al. An efficient control of Curie temperature T_C in Ni-Mn-Ga alloys. J Magn Magn Mater, 2004, 272–276: 2067–2068
11 Wang H B, Chen F, Gao Z Y, et al. Effect of Fe content on fracture behavior of Ni-Mn-Fe-Ga ferromagnetic shape memory alloys. Mater Sci Eng A, 2006, 438–440: 990–993
12 Kikuchi D, Kanomata T, Yamaguchi Y, et al. Magnetic properties of ferromagnetic shape memory alloys $Ni_2Mn_{1-x}Fe_xGa$. J Alloys Compd, 2004, 383: 184–188
13 Ohtsuka M, Matsumoto M, Itagaki K. Effect of iron and cobalt addition on magnetic and shape memory properties of Ni_2MnGa sputtered films. Mater Sci Eng A, 2006, 438–440: 935–939
14 Cai W, Gao L, Liu A L, et al. Martensitic transformation and mechanical properties of Ni-Mn-Ga-Y ferromagnetic shape memory alloys. Scripta Mater, 2007, 57: 659–662
15 Glavatskyy I, Glavatska N, Dobrinsky A, et al. Crystal structure and high-temperature magnetoplasticity in the new Ni-Mn-Ga-Cu magnetic shape memory alloys. Scripta Mater, 2007, 56: 565–568
16 Wang J M, Bai H Y, Jiang C B, et al., A highly plastic $Ni_{50}Mn_{25}Cu_{18}Ga_7$ high-temperature shape memory alloy. Mater Sci Eng A, 2010, 527: 1975–1978
17 Gao L, Cai W, Liu A L, et al. Martensitic transformation and mechanical properties of polycrystalline $Ni_{50}Mn_{29}Ga_{21-x}Gd_x$ ferromagnetic shape memory alloys. J Alloys Compd, 2006, 425: 314–317
18 Tsuchiya K, Tsutsumi A, Ohtsuka H, et al. Modification of Ni-Mn-Ga ferromagnetic shape memory alloy by addition of rare earth elements. Mater Sci Eng A, 2004, 378: 370–376
19 Yu S Y, Cao Z X, Ma L, et al. Realization of magnetic field-induced reversible martensitic transformation in NiCoMnGa alloys. Appl Phys Lett, 2007, 91: 102507-102507-3
20 Sánchez-Alarcos V, Pérez-Landazábal, J I, Recarte V, et al. Correlation between composition and phase transformation temperatures in Ni-Mn-Ga-Co ferromagnetic shape memory alloys. Acta Mater, 2008, 56: 5370–5376
21 Glavatskyy I, Glavatska N, Soderberg O, et al. Transformation temperatures and magnetoplasticity of Ni-Mn-Ga alloyed with Si, In, Co or Fe. Scripta Mater, 2006, 54: 1891–1895
22 Wu G H, Wang W H, Chen J L, et al. Magnetic properties and shape memory of Fe-doped $Ni_{52}Mn_{24}Ga_{24}$ single crystals. Appl Phys Lett, 2002, 80: 634–636
23 Jin X, Marioni M, Bono D, et al. Empirical mapping of Ni-Mn-Ga properties with composition and valence electron concentration. J Appl Phys, 2002, 91: 8222–8224
24 Craciunescu C, Kishi Y, Lograsso T A, et al. Martensitic transforma-

tion in Co_2NiGa ferromagnetic shape memory alloys. Scripta Mater, 2002, 47: 285–288
25 Kokorin V V, Kozlova L E, Titenko A N. Temperature hysteresis of martensite transformation in aging Cu-Mn-Al alloy. Scripta Mater, 2002, 47: 499–502
26 Cong D Y, Wang S, Wang Y D, et al. Martensitic and magnetic transformation in Ni-Mn-Ga-Co ferromagnetic shape memory alloys. Mater Sci Eng A, 2008, 473: 213–218
27 Lanska N, Soderberg O, Sozinov A, et al. Composition and temperature dependence of the crystal structure of Ni-Mn-Ga alloys. J Appl Phys, 2004, 95: 8074–8078
28 Wedel B, Suzuki M, Murakami Y, et al. Low temperature crystal structure of Ni-Mn-Ga alloys. J Alloys Compd, 1999, 290: 137–143
29 James R D, Hane K F. Martensitic transformations and shape-memory materials. Acta Mater, 2000, 48: 197–222
30 Feng Y, Sui J H, Chen L, et al. Martensitic transformation behaviors and magnetic properties of Ni-Mn-Ga rapidly quenched ribbons. Materials Lett, 2009, 63: 965–968
31 Dong G F, Cai W, Gao Z Y, et al. Effect of isothermal ageing on microstructure, martensitic transformation and mechanical properties of $Ni_{53}Mn_{23.5}Ga_{18.5}Ti_5$ ferromagnetic shape memory alloy. Scripta Mater, 2008, 58: 647–650
32 Dong G F, Cai W, Gao Z Y, et al. Effect of isothermal ageing on microstructure, martensitic transformation and mechanical properties of $Ni_{53}Mn_{23.5}Ga_{18.5}Ti_5$ ferromagnetic shape memory alloy. Scripta Mater, 2008, 58: 647–650
33 Webster P J, Ziebeck K R, Town S L, et al. Magnetic order and phase transformation in Ni_2MnGa. Phys Rev B, 1984, 49: 295–310
34 Zheng H X, Xia M X, Liu J, et al. Martensitic transformation of $(Ni_{55.3}Fe_{17.6}Ga_{27.1})_{(100-x)}Co_x$ magnetic shape memory alloys. Acta Mater, 2005, 53: 5125–5129
35 Jiang C B, Feng G, Xu H B. Co-occurrence of magnetic and structural transitions in the Heusler alloy $Ni_{53}Mn_{25}Ga_{22}$. Appl Phys Lett, 2002, 80: 1619–1621